Molecular Therapy
Nucleic Acids
Original Article

RNA-Based Therapy Utilizing Oculopharyngeal Muscular Dystrophy Transcript Knockdown and Replacement

Aida Abu-Baker,[1,10] Nawwaf Kharma,[2,3,10] Jonathan Perreault,[4] Alanna Grant,[1] Masoud Shekarabi,[5] Claudia Maios,[7,8] Michele Dona,[1] Christian Neri,[6] Patrick A. Dion,[1] Alex Parker,[7,8] Luc Varin,[3] and Guy A. Rouleau[1,9]

[1]Montreal Neurological Institute and Hospital, McGill University, Montreal, QC H3A2B4, Canada; [2]Electrical & Computer Engineering Department, Concordia University, 1455 boulevard de Maisonneuve O., Montreal, QC H3G 1M8, Canada; [3]Biology Department, Concordia University, 7141 rue Sherbrooke O., Montreal, QC H4B 1R6, Canada; [4]INRS-Institut Armand-Frappier, 531 boulevard des Prairies, Laval, QC H7V 1B7, Canada; [5]Department of Neuroscience, Center for Neurobiology, Temple University School of Medicine, 3500 N. Broad Street, Philadelphia, PA 19140, USA; [6]INSERM, Laboratory of Neuronal Cell Biology and Pathology, Center for Psychiatry and Neuroscience UMR 894 and University of Paris Descartes, Equipe d'accueil 4059, 75014 Paris, France; [7]CHUM Research Center, Montreal, QC H2X 3H8, Canada; [8]Department of Neuroscience, University of Montreal, Montreal, QC H3T 1J4, Canada; [9]Department of Neurology and Neurosurgery, McGill University, Montreal, QC, Canada

Oculopharyngeal muscular dystrophy (OPMD) is caused by a small expansion of a short polyalanine (polyAla) tract in the poly(A)-binding protein nuclear 1 protein (PABPN1). Despite the monogenic nature of OPMD, no treatment is currently available. Here we report an RNA replacement strategy that has therapeutic potential in cell and *C. elegans* OPMD models. We develop selective microRNAs (miRNAs) against PABPN1, and we report that miRNAs and our previously developed hammerhead ribozymes (hhRzs) are capable of reducing the expression of both the mRNA and protein levels of *PABPN1* by as much as 90%. Since OPMD derives from a very small expansion of GCG within the polyAla tract, our hhRz and miRNA molecules cannot distinguish between the wild-type and mutant mRNAs of *PABPN1*. Therefore, we designed an optimized-codon wild-type PABPN1 (opt-PABPN1) that is resistant to cleavage by hhRzs and miRNAs. Co-expression of opt-PABPN1 with either our hhRzs or miRNAs restored the level of PABPN1, concomitantly with a reduction in expanded *PABPN1*-associated cell death in a stable C2C12 OPMD model. Interestingly, knockdown of the *PABPN1* by selective hhRzs in the *C. elegans* OPMD model significantly improved the motility of the PABPN1-13Ala worms. Taken together, RNA replacement therapy represents an exciting approach for OPMD treatment.

INTRODUCTION

Oculopharyngeal muscular dystrophy (OPMD) is a midlife adult-onset hereditary disease that affects skeletal muscles.[1] It is characterized by progressive swallowing difficulties, eyelid drooping, and serious proximal limb weakness. The pathological hallmark of the disease is the presence of intranuclear inclusions (INIs) in the muscle biopsies of patients.[2,3] In 1990, we began collecting samples from affected families, and, in 1998, we identified the poly(A)-binding protein nuclear 1 protein (*PABPN1*) gene as causative.[4,5] The normal *PABPN1* gene has a $(GCN)_6$ repeat encoding a polyalanine (polyAla) stretch at its 5′ end, while the mutated form observed in OPMD has an expanded repeat $(GCN)_{7-13}$.[4]

Currently there is no effective treatment for OPMD. Since our publication of the first PABPN1 mutations in 1998,[4] several molecular mechanisms have been proposed to contribute to the pathogenesis of the disease,[6] including defects in the potential clearance pathway of the misfolded protein (i.e., chaperones and ubiquitin-proteasome pathway [UPP]),[7] alterations in histone acetylation,[8,9] perturbation in the Wnt signaling pathway,[10] and the role of protein's structure.[11,12] Over the last few years, several potential treatment strategies have emerged targeting these mechanisms.[8,10,13–19] The strategies include drug,[6,8–10,13,14,17,18] cell,[19] and gene therapy[20] (Table S1). Although the role of protein aggregates in OPMD pathogenesis is controversial, drug therapies aiming to reduce misfolded aggregates have been proven effective in pre-clinical studies. For example, chaperone expression,[7,21] 6-aminophenanthridine and guanabenz,[22] ADAPT-232 (Chisan),[6] cystamine,[16] doxycycline,[18] and trehalose[17] have shown phenotype improvement in cell, fly, and mouse models of OPMD. It is noteworthy to mention that disaccharide trehalose is under phase IIb clinical trial for OPMD patients (ClinicalTrials.gov: NCT02015481).[23] Other promising drug therapies, such as lithium chloride,[10] valproic acid,[9] and sirtinol,[8] reduced the cell death without reducing the proportion of cells with aggregates in cellular and worm models of OPMD, possibly by targeting the soluble toxic of $_{exp}$PABPN1.

Received 2 June 2018; accepted 10 February 2019;
https://doi.org/10.1016/j.omtn.2019.02.003.

[10]These authors contributed equally to this work.

Correspondence: Guy A. Rouleau, Montreal Neurological Institute and Hospital, McGill University, 1033 Pine Avenue, Montreal, QC H3A2B4, Canada.
E-mail: guy.rouleau@mcgill.ca

A cell therapy proved to be useful in OPMD patients. A clinical trial was completed recently (ClinicalTrials.gov: NCT00773227),[19] in which grafting of autologous myoblasts isolated from unaffected muscles into the esophagus of the patient showed an improvement in an 80-mL swallowing test. It is important to mention that, although it achieved some short-term efficacy, the transplanted cells still carried the genetic defect.[19]

Gene therapy provides a treatment option for OPMD. A recent study of intramuscular adeno-associated virus (AAV)-mediated gene therapy in an OPMD mouse model showed that silencing the mutated $_{exp}$PABPN1 using small hairpin RNAs (shRNAs) while overexpressing a human codon-optimized normal PABPN1 resistant to the degradation by the shRNAs substantially reduced the amount of insoluble aggregates, decreased muscle fibrosis, reverted muscle strength to the level of healthy muscles, and normalized the muscle transcriptome.[20] Based on this evidence, a pre-clinical study is ongoing in sheep, and a new clinical trial of gene therapy for OPMD patients will be initiated in 2019 by Axovant using the same AAV-mediated gene therapy approach[20] (Table S1).

The development of gene-based therapies for OPMD should benefit from the fact that a single gene is the cause of the disease, and mutations within this gene are always expansion of its alanine-coding repeat. In theory, agents that reduce the level of the mutant PABPN1 should alleviate the disease. Such reduction might be achieved using RNA molecules (e.g., ribozymes and microRNAs) that target mRNA and inhibit expression of the disease gene.[16] Ribozymes are RNA molecules with enzymatic activity that recognize specific RNA sequences and catalyze a site-specific phosphodiester bond cleavage within the target molecule.[24,25] The structure of hammerhead ribozymes consists of two regions of antisense RNA (referred to as the flanking complementarity regions) that flank the nucleolytic motif and provide the target specificity. There exist many types of ribozymes,[26] but the most studied for therapeutic applications are hammerhead ribozymes.[25] MicroRNAs (miRNAs) are small, highly conserved non-coding RNA molecules involved in the regulation of gene expression.[27] miRNAs undergo multiple processing events to reach their functional ~22-ribonucleotide RNA sequence.[28] The nascent miRNA transcripts, which can be more than 1,000 nt in length, contain an shRNA and undergo two cleavage events to form mature miRNA. In the first, the nascent miRNA transcripts are processed into ~60- to 100-nt precursors (pre-miRNA); in the second event that follows, this precursor (a double-stranded RNA arising from small hairpins within RNA) is cleaved to generate ~22-nt mature miRNAs.[27] The miRNAs combine with proteins, shared with the RNAi pathway, to form a complex that binds to mRNA molecules and inhibits their translation.[29] Together with the RNA-induced silencing complex (RISC), miRNAs mediate post-transcriptional gene regulation of their targets, mostly through a sequence complementarity within the 3′ UTR of mRNAs, which reduces translation or causes mRNA degradation.[29] Therefore, silencing is accomplished through a combination of translational repression and mRNA destabilization.[30]

In a recent study, we developed RiboSoft software, which implements a comprehensive hammerhead ribozyme (hhRz) design procedure, and we were able to choose, assay, and validate four ribozymes targeting wild-type *PABPN1* transcript: hhRz144, hhRz363, hhRz437, and hhRz867.[31] These four hhRzs were successfully tested *in vitro* (HEK293T) for their ability to cleave the targeted transcript.[6,31] Because these RNA molecules cannot distinguish between wild-type and mutant PABPN1 RNAs, we decided to develop an opt-PABPN1 that is resistant to cleavage by these RNA molecules. Here we investigate whether concomitant treatments of either hhRzs or newly designed miRNAs (Figures 1, S1, and S2) together with opt-PABPN1 could inhibit PABPN1 expression, in three mammalian cell lines, HeLa, HEK293T, and C2C12, and alleviate the sign of the disease in cellular and worm OPMD models. Interestingly, treatment of nematodes with hhRzs significantly improved the motility of the PABPN1-13Ala worms. Furthermore, we observed cell death reduction in a stable C2C12 OPMD model when hhRzs/miRNAs were co-delivered with the opt-PABPN1.

Our observations, together with those recently reported by Malbera et al.,[20] provide evidence that RNA-based combinatorial therapy could be an effective treatment strategy for OPMD.

RESULTS

No Common SNP Is Associated with the polyAla Repeat Expansion in OPMD

Allele-specific silencing using RNA molecules such as small interfering RNAs (siRNAs), hhRzs, and miRNAs targeting heterozygous SNPs can be a promising therapy for genetic diseases, such as OPMD. Therefore, we first screened the NCBI SNP database searching for a unique SNP associated with *PABPN1*. *PABPN1* links to a total of 2,351 SNPs (https://www.ncbi.nlm.nih.gov/SNP/snp_ref.cgi?locusId=8106) (Table S2). We then searched the literature trying to find any SNP that is associated with the mutated allele. We found four studies reported the presence of specific SNPs that are associated with the polyAla repeat expansion in OPMD[32–35] (Table S3). There are two major limitations of these studies. The first limitation is the lack of a common SNP among different populations of OPMD patients in these studies. The second limitation is the small sample size of the recruited OPMD patients in these studies (Table S3).

Unfortunately, no one SNP has yet been identified that would allow for the specific silencing of the mutant *PABPN1* allele in all patients with OPMD. Therefore, the clinical application of allele-specific targeting may require the development of unique inhibitory RNA sequences on a patient-by-patient basis. Based on these findings, a non-allele-specific therapeutic approach may be feasible as a first-generation therapeutic strategy for the treatment of OPMD. Therefore, we devised a new RNA-based therapy: a combination therapy utilizing hhRz and miRNA knockdown and opt-PABPN1 for the rescue of OPMD.

hhRzs Are Effective in *In Vivo* Transgenic *C. elegans* OPMD Model

On the basis of our earlier findings in HEK293T cells,[31] we decided to test the effectiveness of the three hhRzs (i.e., hhRz144, hhRz363, and

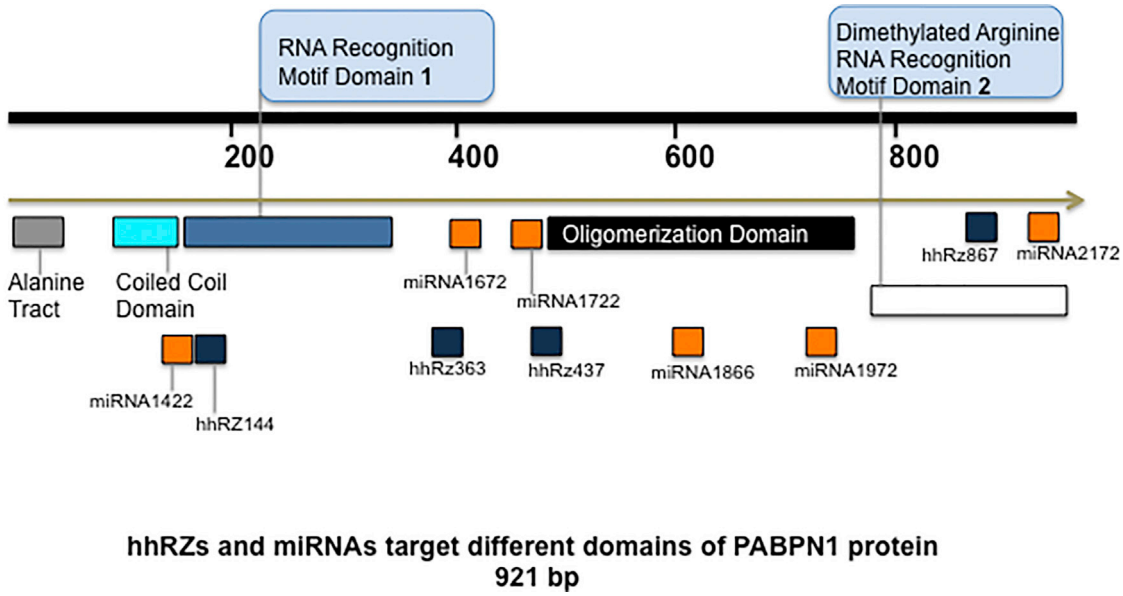

Figure 1. hhRzs and miRNAs Target Different PABPN1 Domains

A schematic representation of human PABPN1 protein showing several domains: polyalanine stretch, proline-rich region, coiled-coil domain, oligomerization domains, and two RNA-binding domains. The figure shows the exact location of each hhRz and miRNAs targeting the different domains of PABPN1.

hhRz437) that achieved the highest silencing effects of PABPN1 in an *in vivo* model of OPMD. We used our previously reported OPMD model of *C. elegans* expressing human PABPN1 with 0 or 13Ala.[8] Each of the three hhRzs was separately inserted into an expression vector (pCFJ594-pENTR) compatible with *C. elegans*; the expression vectors were sent to Knudra Transgenics (Murray, UT, USA) where mos1-mediated single copy insertion (MosSCI) transgenics were generated by transgenic capture (see the Materials and Methods). When the three hhRz nematode plates were established, homozygosity was confirmed by PCR, and each strain expressing a specific hhRz was crossed with the PABPN1 strains (GFP-$_{exp}$PABPN1-13Ala and GFP-PABPN1-0Ala). The descendants of these matings were genotyped to confirm the presence of both *PABPN1* and the hhRz transgenes.

To test the silencing effect of hhRz on PABPN1 level in this model, we first measured the level of PABPN1 knockdown by western blot immune detections. We confirmed that the protein levels of PABPN1 were markedly reduced in PABPN1-13Ala animals crossed with any one of the three hhRzs compared to non-crossed PABPN1-13Ala animals (Figure 2A). However, this decrease was not obvious in PABPN1-0Ala animals crossed with any one of the three hhRzs. Consistent with the western blot analysis, the fluorescence data analysis showed decreased GFP protein levels in crossed PABPN1-13Ala animals (Figure 2B). This was obvious when we examined the appearance of muscle cells by scoring the number of fluorescent muscle cell nuclei in animals crossed with or without any one of the three hhRzs. A striking GFP signal loss was observed in PABPN1-13Ala animals crossed with hhRz144, hhRz363, or hhRz437 compared to non-crossed PABPN1-13Ala animals (Figure 2B).

The OPMD phenotype of these transgenic nematodes includes adult-stage abnormalities like a reduced motility and the degeneration of muscle cells, and it is only observed in transgenic strains expressing the 13Ala human PABPN1 protein.[8] Therefore, we sought to test the effect of these hhRzs on the motility of these worms. An automated motility tracking system (Microtracker) was used to detect the motion of the worms on a continuous basis. The motility of mutant animals expressing 13Ala human PABPN1 protein declined quickly, such that these animals were completely paralyzed (Figure 2C). On the other hand, a remarkable improvement in motility was observed in PABPN1-13Ala animals crossed with hhRz144, hhRz363, or hhRz437 compared to non-crossed PABPN1-13Ala animals throughout all time points (Figure 2C), reaching the motility level detected in control PABPN1-0Ala animals (Figure 2C). Altogether, this suggests that knockdown of the PABPN1-13Ala alleviates the adult-stage abnormalities in the *C. elegans* OPMD model.

hhRzs and miRNAs Are Potent Inhibitors of PABPN1's Expression

The current study takes advantage of the capacity of RNA molecules to specifically target PABPN1. Overall, the target sites of chosen hhRzs and miRNAs span all the coding sequence of *PABPN1* (Figure 1; Figures S1 and S2). To confirm the capacity of hhRz previously reported[31] to target human *PABPN1* in HEK293T cells in other mammalian cell lines, we tested hhRzs in HeLa and C2C12 cells.

To maximize the results, we decided to design and use miRNAs that would inhibit *PABPN1* transcript in a different mechanism from hhRzs (Materials and Methods). Using RNAi designer (Invitrogen), we designed six selective miRNAs against human *PABPN1*: miRNA1422,

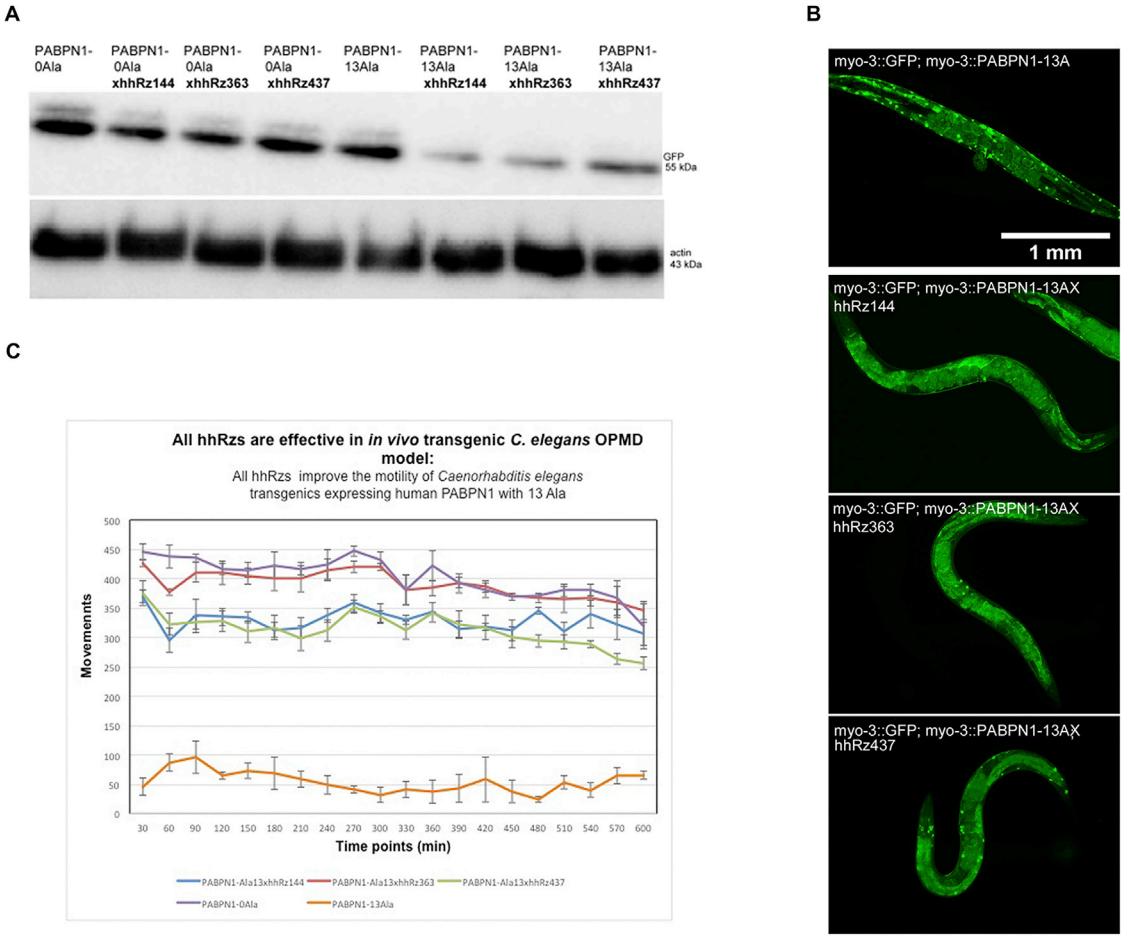

Figure 2. hhRzs Are Effective in *In Vivo* Transgenic OPMD *C. elegans*

(A) Western blot showing the high efficiency of hhRzs in knocking down PABPN1 protein level in OPMD *C. elegans*. PABPN1-13Ala and PABPN1-0Ala animals were crossed with hhRz144, hhRz363, or hhRz437. The crossed animals were then genotyped before protein extraction. The protein levels of PABPN1 were markedly reduced in PABPN1-13 animals crossed with any one of the three hhRzs compared to non-crossed animals. This decrease was not obvious in PABPN1-0Ala animals crossed with any one of the three hhRzs. The immunoblot was performed using GFP antibody. Actin antibody was used to indicate equal loading across all lanes. (B) hhRzs lead to a decrease in GFP signal when crossed with PABPN1-13A animals. The top image shows an adult *C. elegans* expressing myo-3::GFP; myo-3::PABPN1-13A in the nuclei of body-wall muscle cells. The worms in the three images below co-express myo-3::GFP; myo-3::PABPN1-13A with hhRz144, hhRz363, or hhRz437. Expression of hhRz causes fading of the GFP signal, indicating silencing of PABPN1. Scale bar, 1 mm. (C) Knockdown of the PABPN1 alleviates the adult-stage abnormalities in the *C. elegans* OPMD model. The motility of mutant animals expressing 13Ala human PABPN1 protein declined quickly, such that these animals were completely paralyzed. However, a significant improvement in motility was observed in PABPN1-13Ala animals crossed with hhRz144, hhRz363, or hhRz437 compared to non-crossed PABPN1-13Ala animals throughout all time points, reaching the motility level detected in control animals (PABPN1-0Ala) (*$p < 0.0001$). Motility recordings were generated using a Microtracker device, an automated tracking system that detects the animal movement through infrared microbeam light scattering. Simply, each microtiter well is crossed by at least one infrared microbeam, scanned more than 10 times/s. The detected signal is then digitally processed to register the amount of animal movement in a fixed period of time. At the indicated time points, the number of movements was scored at 22°C, for 10 consecutive h.

miRNA1672, miRNA1722, miRNA1866, miRNA1972, and miRNA2172 (Figure S2). We then inserted them in the GFP-miRNAi expression vector, suitable for transient and stable expression in cells (Materials and Methods). The use of a GFP-miRNA backbone vector (Figure S3) provides important advantages over shRNA vectors in minimizing the off-target possibility.[36]

To test the hhRzs' and miRNAs' silencing effects in the three mammalian cell lines, the cells were transfected with the different RNA molecules before we performed real-time qPCR, ELISA, and western blot to assess the effectiveness of these RNA molecules in knocking down endogenous PABPN1 level. We also monitored the number of viable cells treated with different hhRzs and miRNAs in comparison with untreated control cells. This cell survival-tracking assay was done over 7 days using a live-stage microscope in the three cell lines (Figures 3A, 4A, and 5A, the columns without opt-PABPN1). It is worth noting that expressing hhRzs or miRNAs in cells did not cause cellular toxicity at the first 4 days post-transfection

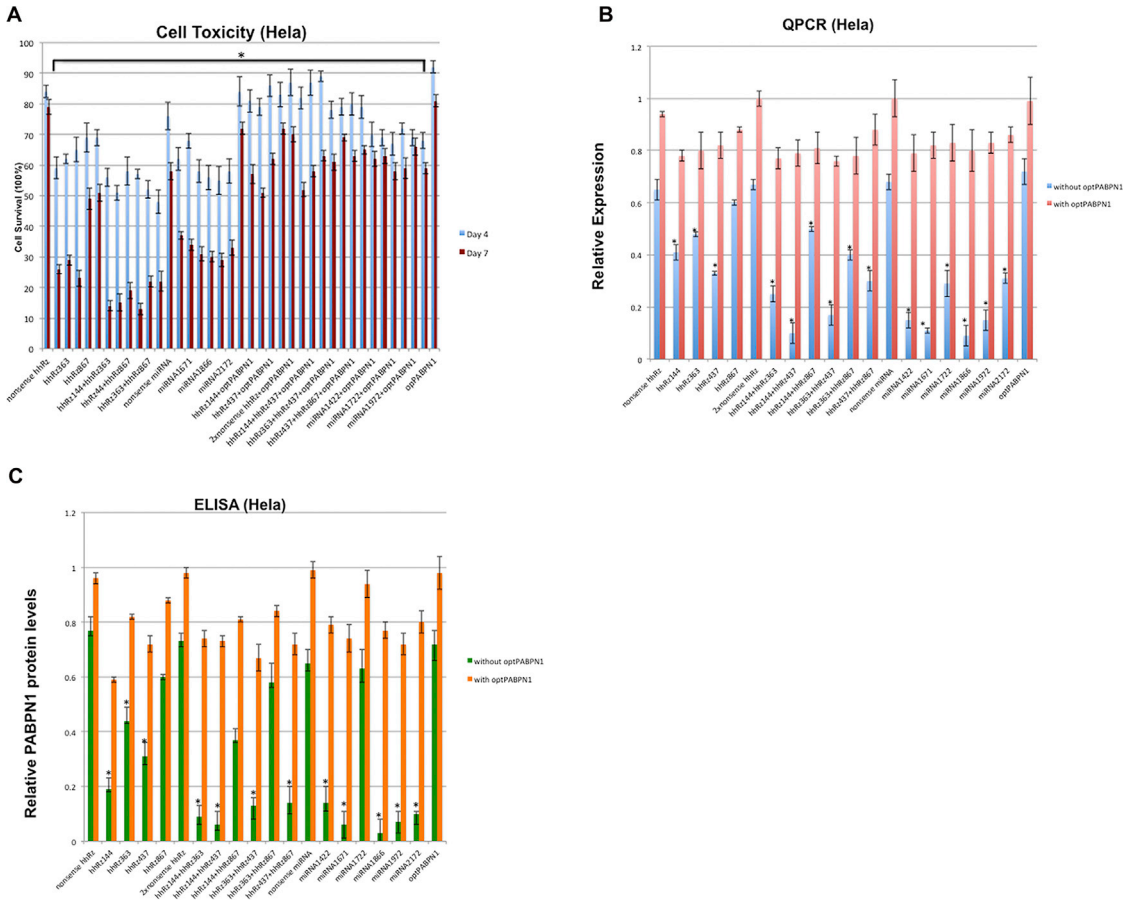

Figure 3. The Effects of hhRz and miRNA Delivery with and without opt-PABPN1 in HeLa Cells

(A) Percentage of cell survival was determined by live-stage microscopy in cells transfected with RNA molecules with or without opt-PABPN1. Co-transfection of opt-PABPN1 (right side of the graph) with hhRzs or miRNAs shows a striking increased percentage of cell survival compared to cells transfected with only hhRzs or miRNAs at different time points (mean ± SE; *$p < 0.001$ versus nontreated samples, ANOVA). (B) Measurement of endogenous *PABPN1* gene expression in the HeLa cells transfected with one hhRz, a combination of two hhRzs, or one miRNA by qPCR. Controls were also included. RNA was collected 48 h post-transfection. qPCR analysis evaluating the endogenous *PABPN1* mRNA levels showed a significant downregulation of *PABPN1* for cells transfected with hhRz144, hhRz363, and hhRz437 with respect to the nonsense hhRz. A substantial reduction of *PABPN1* mRNA levels was detected when HeLa cells were co-transfected with the corresponding two hhRzs. RNA polymerase II served as a normalization control gene. Values are given as means ± SE of three independent experiments and each experiment was performed in triplicate. *$p < 0.005$, $n = 3$. Significant downregulation of human endogenous *PABPN1* mRNA was observed after transfecting HeLa cells with the six different miRNAs targeting PABPN1. *$p < 0.005$, $n = 3$. The figure shows a clear increase in *PABPN1* mRNA levels when opt-PABPN1 was introduced into cells with the hhRzs or miRNAs, indicating that opt-PABPN1 is capable of enhancing *PABPN1* mRNA levels (right side of the graph). (C) ELISA results for PABPN1 show a clear inhibition of endogenous PABPN1 protein following hhRz or miRNA transfection. This inhibition was clearly rescued by co-expressing opt-PABPN1 with hhRzs or miRNAs. Protein levels were measured in supernatants of HeLa 48 h post-transfection. The values represent the means ± SDs from three independent experiments performed in triplicate. *$p < 0.05$ using Student's t test.

(Figure S3); however, cells began to die at a later stage in culture (5–7 days) compared to controls (Figures 3A, 4A, and 5A, the columns without opt-PABPN1; Figure S4).

PABPN1 mRNA levels were analyzed using qPCR to assess the ability of hhRzs and miRNAs to inhibit *PABPN1* at the RNA level in cells (Figures 3B, 4B, and 5B, the columns without opt-PABPN1). When cells were transfected with one single hhRz, *PABPN1* transcript level was clearly inhibited at different days post-transfection in the three cell lines, with hhRz867 yielding the lowest knockdown (Figures 3B, 4B, and 5B, the columns without opt-PABPN1). To achieve more efficient knockdown of *PABPN1* transcript level, we combined two hhRzs together and obtained a stronger knockdown of *PABPN1* mRNA levels. For example, a reduction close to 80% in *PABPN1* RNA level was achieved when cells were co-transfected with two hhRzs, hhRz144 and hhRz437 (Figures 3B, 4B, and 5B, the columns without opt-PABPN1). In addition, we tested the ability of miRNAs to knock down *PABPN1*. While miRNA1722 and miRNA2172 achieved ~60% inhibition of *PABPN1* transcript level, by day 2 post-transfection in cells, we noted a comparable ~90% reduction in *PABPN1* transcript level of cells treated with miRNA1422, miRNA1672, miRNA1866, and miRNA1972 in three cell lines

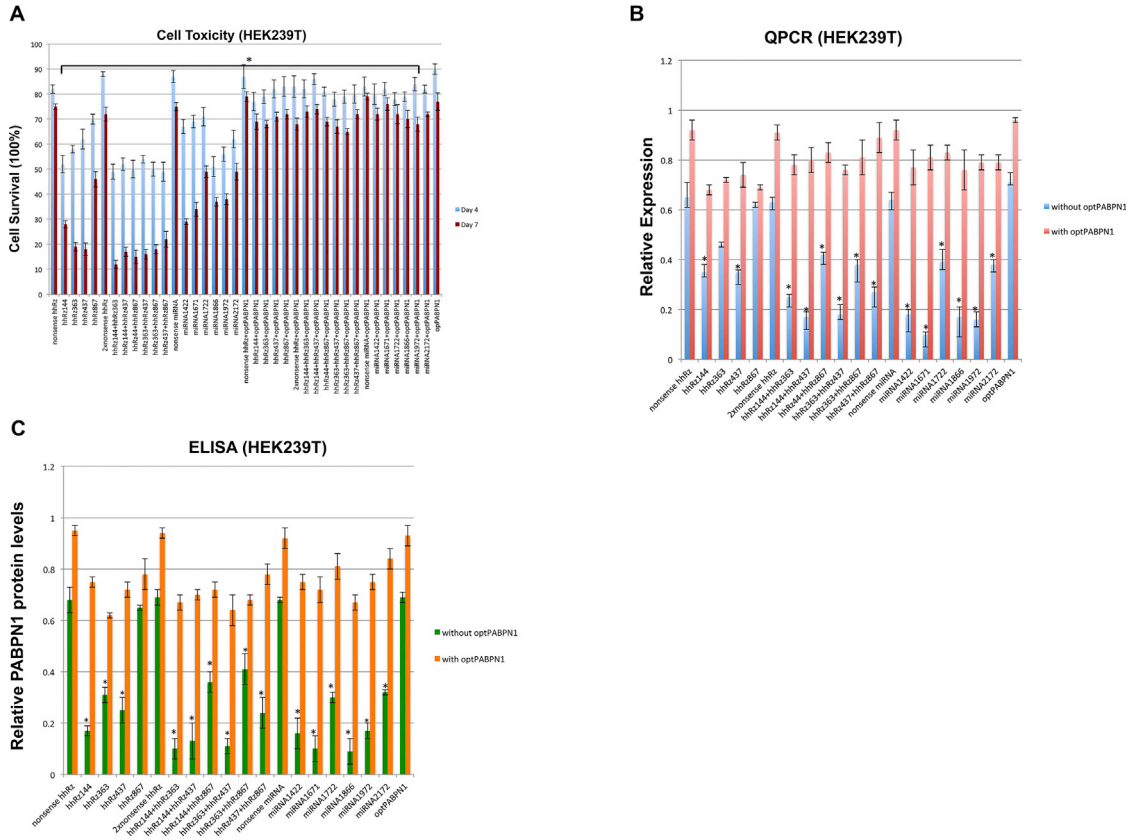

Figure 4. The Effects of hhRz and miRNA Delivery with and without opt-PABPN1 in HEK239T Cells

(A) Percentage of cell survival was determined by live-stage microscopy in cells transfected with RNA molecules with or without opt-PABPN1. Co-transfection of opt-PABPN1 (right side of the graph) with hhRzs or miRNAs shows a striking increased percentage of cell survival compared to cells transfected with hhRzs or miRNAs but without opt-PABPN1 at different time points (mean ± SE; *$p < 0.001$ versus nontreated samples, ANOVA). (B) Measurement of endogenous *PABPN1* gene expression in the HEK239T cells transfected with individual hhRz, a combination of two hhRzs, or individual miRNA by qPCR. Controls were also included. RNA was collected 48 h post-transfection. qPCR analysis evaluating the endogenous *PABPN1* mRNA levels showed a significant downregulation of *PABPN1* for cells transfected with hhRz144, hhRz363, and hhRz437 with respect to the nonsense hhRz. A substantial reduction of *PABPN1* mRNA levels was detected when HEK239T cells were co-transfected with the corresponding two hhRzs. RNA polymerase II served as a normalization control gene. Values are given as means ± SE of three independent experiments and each experiment was performed in triplicate. *$p < 0.005$, $n = 3$. Significant downregulation of human endogenous *PABPN1* mRNA was observed after transfecting HEK239T cells with the six different miRNAs targeting *PABPN1*. *$p < 0.005$, $n = 3$. The figure shows a clear increase in *PABPN1* mRNA levels when opt-PABPN1 was co-transfected with RNA molecules, indicating that opt-PABPN1 is capable of enhancing *PABPN1* mRNA levels (right side of the graph). (C) ELISA results for PABPN1 show a clear inhibition of endogenous PABPN1 protein following hhRz or miRNA transfection. This inhibition was clearly rescued by co-expressing opt-PABPN1 with hhRzs or miRNAs. Protein levels were measured in supernatants of HEK239T 48 h post-transfection. The values represent the means ± SDs from three independent experiments performed in triplicate. *$p < 0.05$ using Student's t test.

(Figures 3B, 4B, and 5B, the columns without opt-PABPN1). Because these individual miRNAs achieved effective knockdown of the *PABPN1* mRNA, it was not necessary to perform the experiments of combined miRNAs.

To verify whether the downregulation observed at the RNA level translated into a downregulation at protein level, we performed ELISAs. A similar reduction was observed in intracellular PABPN1 protein levels assayed by ELISA in the three cell lines (Figures 3C, 4C, and 5C, the columns without opt-PABPN1), with some observed differences among them, particularly for miRNA1722. Therefore, our hhRzs and miRNAs were effective at inhibiting PABPN1's expression. We further confirmed our results and performed western blot to analyze PABPN1 protein levels (Figures S5–S7).

Developing the opt-PABPN1

Based on our promising results, we were encouraged to pursue this RNA-based strategy and optimize the relevant therapy for OPMD. It is known that most OPMD patients are heterozygous at the OPMD locus, carrying one mutant and one wild-type allele. Although mutant PABPN1 protein is toxic to muscles, its wild-type counterpart is protective against apoptotic muscle death.[37] An effective gene therapy must silence the deleterious mutant allele without eliminating expression of the beneficial wild-type one. As the mutation in

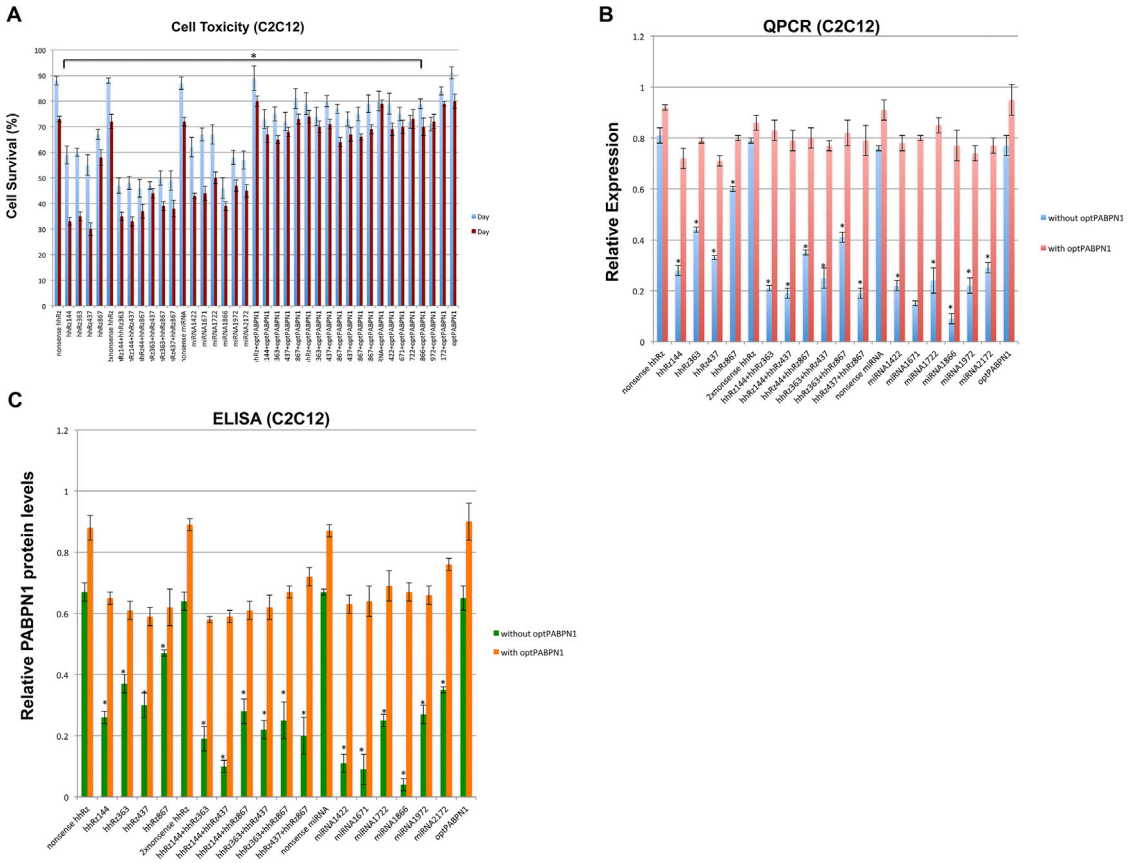

Figure 5. The Effects of hhRz and miRNA Delivery with and without opt-PABPN1 in C2C12

(A) Percentage of cell survival was determined by live-stage microscopy in cells transfected with RNA molecules with or without opt-PABPN1. Co-transfection of opt-PABPN1 (right side of the graph) with hhRzs or miRNAs shows a striking increased percentage of cell survival compared to cells transfected with hhRzs or miRNAs but without opt-PABPN1 at different time points (mean ± SE; *$p < 0.001$ versus nontreated samples, ANOVA). (B) Measurement of endogenous *PABPN1* gene expression in the C2C12 cells transfected with individual hhRz, a combination of two hhRzs, or individual miRNA by qPCR. Controls were also included. RNA was collected 48 h post-transfection. qPCR analysis evaluating the endogenous *PABPN1* mRNA levels showed a significant downregulation of *PABPN1* for cells transfected with hhRz144, hhRz363, and hhRz437 with respect to the nonsense hhRz. A substantial reduction of *PABPN1* mRNA levels was detected when C2C12 cells were co-transfected with the corresponding two hhRzs. RNA polymerase II served as a normalization control gene. Values are given as means ± SE of three independent experiments and each experiment was performed in triplicate. *$p < 0.005$, $n = 3$. Significant downregulation of human endogenous *PABPN1* mRNA was observed after transfecting C2C12 cells with the six different miRNAs targeting *PABPN1*. *$p < 0.005$, $n = 3$. The figure shows a clear increase in *PABPN1* mRNA levels when opt-PABPN1 was co-transfected with hhRzs or miRNAs, indicating that opt-PABPN1 is capable of enhancing *PABPN1* mRNA levels (right side of the graph). (C) ELISA results for PABPN1 show a clear inhibition of endogenous PABPN1 protein following hhRz or miRNA transfection. This inhibition was clearly rescued by co-expressing opt-PABPN1 with these RNA molecules. Protein levels were measured in supernatants of C2C12 48 h post-transfection. The values represent the means ± SDs from three independent experiments performed in triplicate. *$p < 0.05$ using Student's t test.

OPMD is a very small expansion of GCG within an alanine tract, RNA-targeting molecules cannot distinguish between wild-type and mutant *PABPN1* RNAs. Introduction of the molecule into cells would cause the cleavage and degradation of all endogenous *PABPN1* transcripts.

To achieve a successful gene therapy, the replacement gene sequence would need to be altered in such a way as to render it unique from the hhRz/miRNA recognition sequences. Therefore, we decided to develop an opt-PABPN1 that is resistant to cleavage by these RNA molecules (Materials and Methods). Gene optimization takes advantage of the degeneracy of the genetic code. Because of degeneracy, one protein can be encoded by many alternative nucleic acid sequences. Here we changed the nucleotide sequence of *PABPN*1 cDNA to give different codons, keeping the same amino acid sequence of the PABPN1 protein (Figure S8). The percent of nucleotide sequence identity between wild-type PABPN1 and opt-PABPN1 is 75%, yet the amino acid identity is 100% (Figure S8). It is important to mention that we changed the whole sequence and not just the target sequences for the hhRzs and miRNAs. cDNA sequence was also modified to include an optimum consensus Kozak sequence for translation initiation (Invitrogen; Figure S9), and GC content was

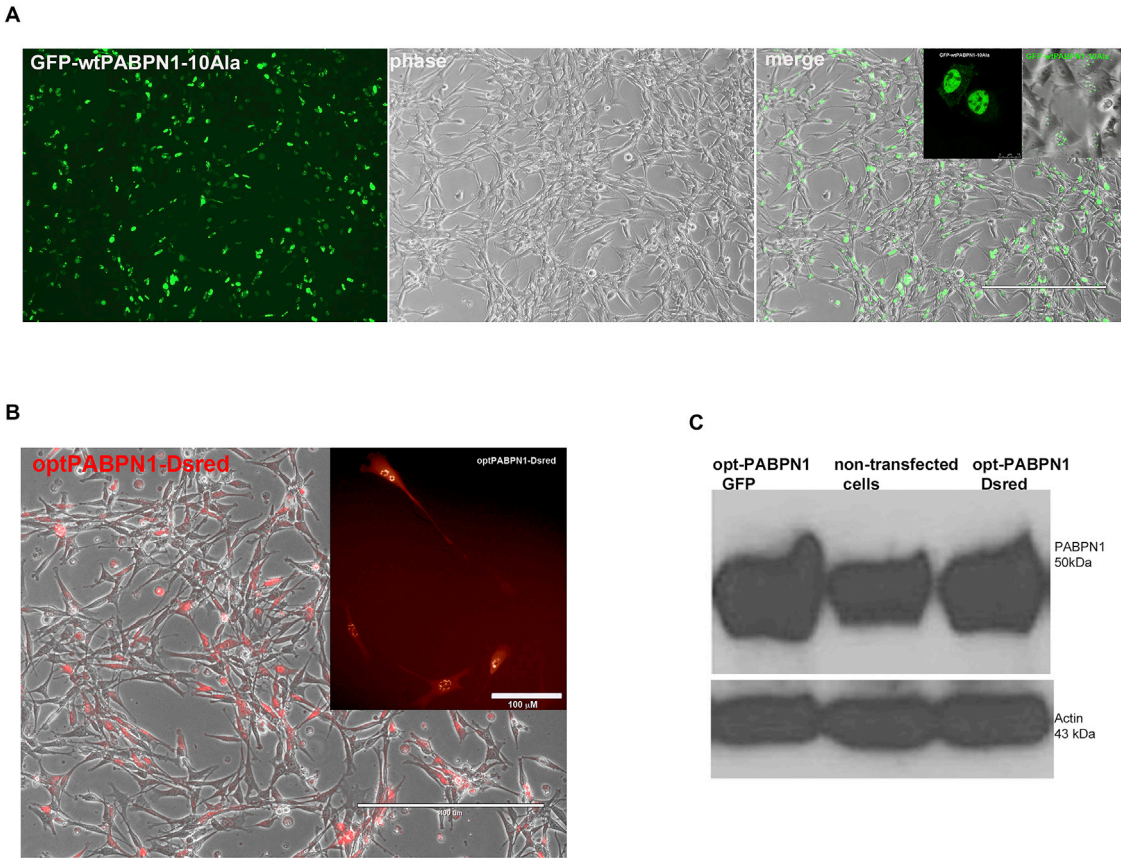

Figure 6. Developing the opt-PABPN1 that Is Resistant to Knockdown by the hhRzs and miRNAs

(A) Subcellular localization of wild-type PABPN1. C2C12 cells were transfected with GFP-wild-type (WT)-PABPN1-10Ala and visualized under the fluorescent microscope 48 h post-transfection. Wild-type PABPN1 is a nuclear protein with widespread staining in the nucleoplasm. It is mostly concentrated in discrete nuclear domains called speckles. Phase images are also shown. (B) Cellular expression of opt-PABPN1 is similar to wild-type PABPN1-10Ala. Fluorescent microscopic images show the subcellular expression of opt-PABPN1-Dsred. C2C12 cells were transiently transfected with the opt-PABPN1-Dsred. Images were captured 48 h post-transfection using a fluorescent microscope. Scale bars are indicated. (C) opt-PABPN1 enhances protein expression. As shown by western blot, there was a clear increase in the level of PABPN1 expression after opt-PABPN1 transfection. The level of PABPN1 expression is higher in lane 1 (opt-PABPN1-GFP) and in lane 3 (opt-PABPN1-Dsred) compared to lane 2 (non-transfected cells). The proteins were then extracted at 48 h after transfection. PABPN1 antibody was used to measure PABPN1 protein level. The actin expression is used to indicate equal loading across all lanes.

increased to promote RNA stability (Invitrogen; Figure S9). Thus, the *PABPN1* cDNA sequence was optimized in a number of ways to improve mRNA stability and translation efficiency and, more importantly, to be resistant to degradation by hhRzs/miRNAs.

opt-PABPN1 Is Resistant to Any Degradation Caused by hhRzs or miRNAs

First, we tested the ability of the opt-PABPN1 to mediate enhanced transgene expression. Wild-type PABPN1 is an abundant nuclear protein, with widespread staining in the nucleoplasm as shown in C2C12 transfected with wild-type PABPN1-GFP (Figure 6A). It is mostly concentrated in discrete nuclear domains called speckles[38–40] (Figure 6A). We examined the expression of opt-PABPN1-GFP and opt-PABPN1-Dsred using the fluorescent microscope. As expected, cells expressing opt-PABPN1 showed a cellular localization similar to wild-type PABPN1, with abundant nuclear expression and the presence of nuclear speckles as a distinct feature of PABPN1 (Figure 6B). We then detected the PABPN1 levels by western blot. The opt-PABPN1 resulted in a clear increase in PABPN1 protein level compared with control samples (Figure 6C).

We have tested hhRzs alone and in combination in our previous study,[31] but without the opt-PABPN1. Here we tested the effect of opt-PABPN1 when co-expressed with hhRzs or miRNAs on the cell toxicity and mRNA and protein expressions of PABPN1 in the three cell lines. Critically, when opt-PABPN1 was introduced into the cells simultaneously with one hhRz, with a combination of two hhRzs, or with one miRNA, the cell death was prevented (Figures 3A, 4A, and 5A, the columns with opt-PABPN1). Using a selective probe for opt-PABPN1 as well as specific primers for opt-PABPN1 (Figure S8; Materials and Methods), the expression of opt-PABPN1 appeared unchanged at the mRNA levels, as detected by qPCR (Figures 3B,

4B, and 5B, the columns with opt-PABPN1). Moreover, there was no noticeable decrease in protein levels of PABPN1, as detected by ELISA when hhRzs/miRNAs were co-transfected with opt-PABPN1 (Figures 3C, 4C, and 5C, the columns with opt-PABPN1). We further confirmed our ELISA results and performed immunoblotting to analyze PABPN1 protein levels (Figures S10–S12).

Co-transfection of opt-PABPN1 with hhRzs/miRNAs Increases Cell Survival in the OPMD Cell Model

We previously developed a stable C2C12 cell model that is relevant to OPMD.[6,9] We sought to evaluate the silencing effects of hhRzs and miRNAs, with or without the opt-PABPN1, in this model. Our established stable C2C12 model allowed us to assess the effect of these RNA molecules on cell survival over a long period. First, we analyzed the cell survival when hhRzs were delivered with or without opt-PABPN1 in C2C12-17Ala myoblasts (a stable cell line transfected with GFP-$_{exp}$PABPN1-17Ala) (Figure 7A). Similarly, we analyzed the cell survival when miRNAs were delivered with or without opt-PABPN1 in C2C12-17Ala myoblasts (Figure 7B). We monitored the cell morphology and survival using a live-stage microscope for a period of 10 days.[6,9,10] Co-expressing opt-PABPN1 with hhRzs/miRNAs showed consistent and significant protective effects against induced cell death associated with $_{exp}$PABPN1-17Ala in these myoblasts, compared to the non-transfected counterparts at different time points (Figure 7C). It is important to mention that transfecting the RNA molecules (i.e., hhRZs/miRNAs) alone in cells, without opt-PABPN1, could not protect against the cell death (Figures 7A–7C). We looked at nuclear morphology to determine cell viability, and GFP-expressing cells with fragmented or condensed nuclei were counted as dead.[6,10] While increased cell death with a progressive loss of green living cells was observed in all cells expressing C2C12-17Ala treated with the RNA molecules over the time course, co-expression of opt-PABPN1 with the RNA molecules significantly increased the percentage of living green cells (Figures 7A–7C).

Furthermore, we confirmed the downregulation of mRNA and protein expressions. As expected, the three effective hhRzs, the combined hhRzs, and the four effective miRNAs led to substantial decreases in the RNA and protein levels of PABPN1, as assayed by qPCR, ELISA (Figures 7D and 7E), and western blot (Figures S13–S15). Interestingly, when C2C12-17Ala cells were co-transfected with one of the hhRzs or miRNAs and the opt-PABPN1, the levels of mRNA and protein were restored due to opt-PABPN1 expression (Figures S16–S18). It is important to mention that expressing opt-PABPN1 alone in cell was not enough to protect against the cell death associated with $_{exp}$PABPN1-17Ala, indicating that simultaneous delivery of hhRzs/miRNAs for the clearance of *PABPN1* and opt-PABPN1 for augmentation of wild-type protein is necessary to confer the protection against cell death in C2C12-17Ala myobalsts.

DISCUSSION

Despite the monogenic nature of the disease and the time that has elapsed since the identification of the mutations responsible for OPMD, as well as the progress in understanding the molecular mechanisms, there is no available treatment for patients afflicted with the disease at the moment. Therapy is limited to the management of symptoms. Various surgical approaches can transiently improve swallowing. Ptosis can also be surgically corrected. These procedures do not affect the progression of the disease and the symptoms usually reappear. Here we show a silence-and-replace RNA therapeutic approach for OPMD. Because the mRNA *PABPN1* would be selectively targeted (using RNA molecules) and the normal transcript would remain unaffected (using the opt-PABPN1), the normal functions of PABPN1 that may be critical for muscle function would be maintained.

Here we tested two RNA molecules that bind to *PABPN1* RNA by base pairing in a sequence-specific manner yet have different mechanisms of action and effects. Previously, we tested hhRzs targeting *PABPN1* in HEK293T cells without opt-PABPN1.[31] For a better comparison with other cell lines, here we tested these hhRzs in HeLa, C2C12, and HEK293T cells with or without opt-PABPN1. In addition to hhRzs, we successfully suppressed the expression of *PABPN1*'s transcript using our selective designed miRNAs. RNA molecules (antisense oligonucleotides) are potentially potent and selective agents that can alter target gene expression by binding to RNA.[41] Once bound, these RNA molecules either disable or induce the degradation of the target RNA.[41,42] Our data clearly support the effectiveness of hhRzs, as their biological activities are demonstrated in both *in vitro* and *in vivo* models of OPMD.

Our results show that the knockdown efficiency at the RNA and/or protein level is consistent in HeLa, HEK239T, and C2C12 cells and that hhRz144, hhRz437, miRNA1422, miRNA1671, miRNA1972, and miRNA1866 are optimal candidates for effective knockdown.

Knocking down any endogenous gene can lead to anticipated or unanticipated direct toxicity, owing to non-redundant functions in the normal physiology of the target gene. Our designed miRNAs achieved a long-term knockdown of *PABPN1* in the three cell lines with less cellular toxicity than hhRzs (Figures 3A, 4A, and 5A). It is worth mentioning that artificial miRNAs are processed more efficiently than shRNA, leading to both effective target gene silencing and improved cellular safety.[23,30]

Our exciting results generated from the OPMD worm model support the idea that reducing the levels of mutant allele could be beneficial. It seems that our hhRzs selectively target the $_{exp}$PABPN1-13Ala and not the PABPN1-0Ala in OPMD *C. elegans*. Although we do not know why these hhRzs showed allele preference, one explanation could be that the $_{exp}$PABPN1-13Ala has a more open structure, making it more accessible for hhRz binding, thereby leading to the induction of selective knockdown, resulting in a lower PABPN1 expression. It was previously reported that co-localization of the ribozyme with the target and accessibility of the ribozyme for binding to the target may influence the overall effect.[43]

In this study, we provided an important approach to restore the level of PABPN1 by introducing opt-PABPN1 simultaneously with hhRzs

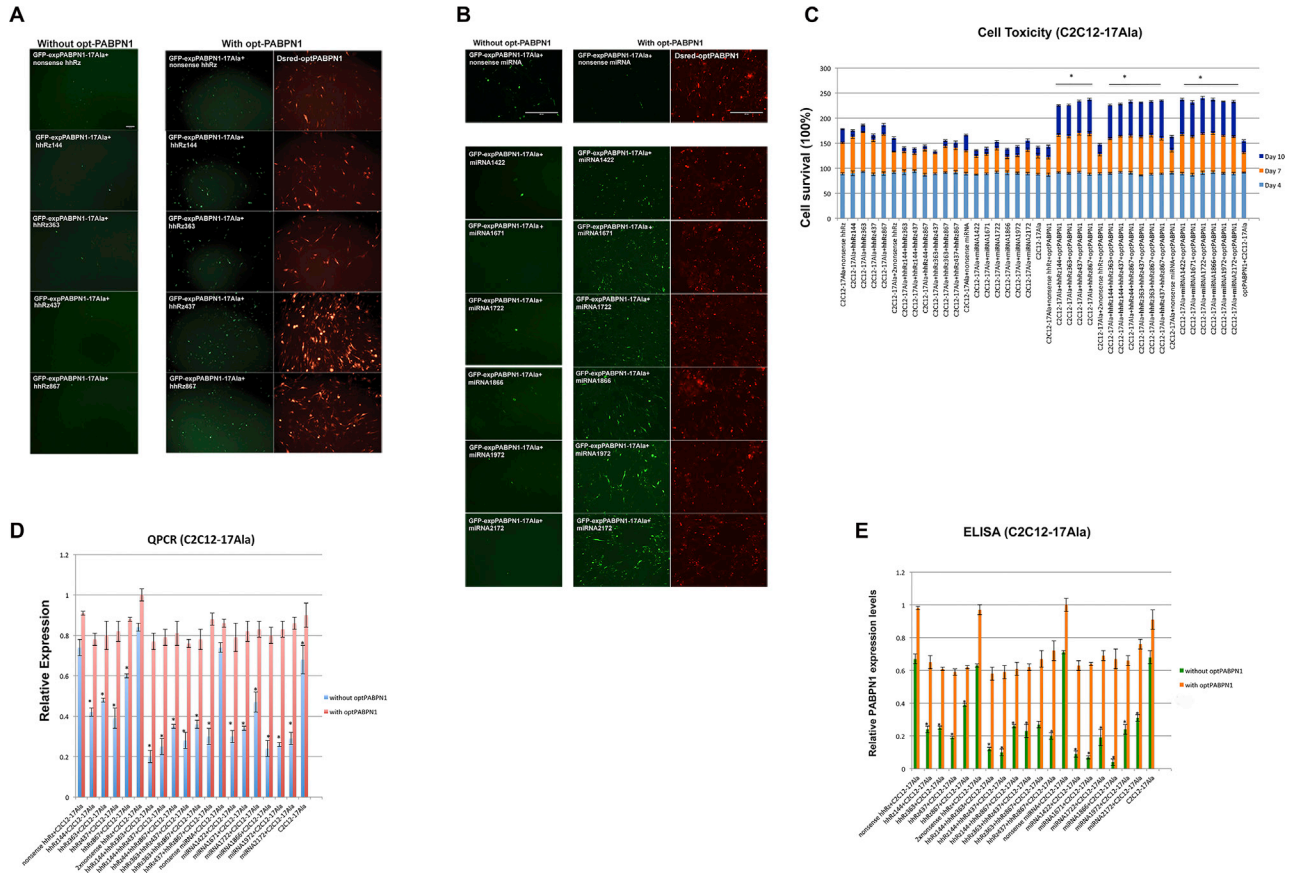

Figure 7. The Effects of hhRz and miRNA Delivery with and without opt-PABPN1 in a Stable C2C12 OPMD Cell Model

(A) Co-transfection of opt-PABPN1 with hhRzs increases the cell survival in C2C12-17Ala myoblasts. Representative images show C2C12-17Ala myoblasts treated with hhRzs with or without opt-PABPN1. PABPN1 knockdown by hhRzs induced significant cell death in C2C12-17Ala myoblasts (left), but co-expressing opt-PABPN1 with hhRzs rescued cells from cell death (right). Cells were monitored using a live-stage microscope every day and up to 14 days in culture. Images were captured at day 10. Scale bar, 100 μM. (B) Co-transfection of opt-PABPN1 with miRNAs increases the cell survival in C2C12-17Ala myoblasts. PABPN1 knockdown by miRNAs induces significant cell death in C2C12-17Ala myoblasts (left). Co-expressing opt-PABPN1 with miRNAs rescued cells from cell death (right). Cells were monitored using a live-stage microscope every day and up to 14 days in culture. Images were captured at day 10. Scale bar, 100 μM. (C) Percentage of cell survival was determined by live-stage microscopy. C2C12-17Ala myoblasts were transfected with hhRzs or miRNAs with or without opt-PABPN1 and monitored at different days in culture. In C2C12-17Ala myoblasts, the cell death started at day 7 of culture and reached its highest point after day 10. Co-transfection of opt-PABPN1 (right side of the graph) with hhRzs or miRNAs shows a striking increased percentage of cell survival compared to cells transfected with only hhRzs or miRNAs at days 7 and 10 in culture (mean ± SE; *$p < 0.001$ versus nontreated samples, ANOVA). It is important to mention that expressing opt-PABPN1 alone in cell was not enough to protect against the cell death associated with $_{exp}$PABPN1-17Ala. (D) Measurement of endogenous *PABPN1* gene expression in the C2C12-17Ala myoblasts transfected with one hhRz, a combination of two hhRzs, or one miRNA by qPCR. Controls were also included. RNA was collected 4 days post-transfection. qPCR analysis evaluating the endogenous *PABPN1* mRNA levels showed a significant downregulation of *PABPN1* for cells transfected with hhRz144, hhRz363, and hhRz437, with respect to the nonsense hhRz. A substantial reduction of *PABPN1* mRNA levels was detected when C2C12-17Ala myoblasts were co-transfected with the corresponding two hhRzs. RNA polymerase II served as a normalization control gene. Values are given as means ± SE of three independent experiments and each experiment was performed in triplicate. *$p < 0.005$, $n = 3$. Significant downregulation of human endogenous *PABPN1* mRNA was observed after transfecting C2C12-17Ala myoblasts with the six different miRNAs targeting PABPN1. *$p < 0.005$, $n = 3$. The figure shows a clear increase in *PABPN1* mRNA levels when opt-PABPN1 was introduced into cells with the hhRzs or miRNAs, indicating that opt-PABPN1 is capable of enhancing *PABPN1* mRNA levels (right side of the graph). (E) ELISA results for PABPN1 show a clear inhibition of endogenous PABPN1 protein following hhRz or miRNA transfection. This inhibition was clearly rescued by co-expressing opt-PABPN1 with hhRzs or miRNAs. Protein levels were measured in supernatants of C2C12-17Ala myoblasts 4 days post-transfection. The values represent the means ± SDs from three independent experiments performed in triplicate. *$p < 0.05$ using Student's t test.

or miRNAs. It is exciting to find out that this RNA therapeutic approach protects against C2C12-17Ala-associated death. This protective effect is likely to be mediated by the anti-apoptotic effects mediated by the miRNA- and hhRz-resistant opt-PABPN1. It was previously shown that an anti-apoptotic function of wild-type PABPN1 is mediated via translational regulation of XIAP, which is a potent anti-apoptotic molecule.[37] These results further support that the codon optimization of the PABPN1 protects against cellular toxicity in OPMD, a feat potentially enhanced by the fact that opt-PABPN1 is more efficiently translated and expressed.

Our current work is in agreement with a recent study on OPMD where combining knockdown of endogenous PABPN1 and its replacement by a wild-type PABPN1 substantially reduced the amount of insoluble aggregates, decreasing muscle fibrosis in a mouse model of OPMD.[20] Interestingly, we were the first to propose this therapeutic approach.[6] This could represent a future avenue for the treatment of numerous inherited diseases for which mutant versions of the gene do not differ enough from the healthy version for reliable specific targeting, such as is the case for OPMD and most other diseases caused by repeat expansions.[44–46]

MATERIALS AND METHODS

Construction of Plasmids for hhRz and miRNA Expression

The DNA sequences of the hhRzs and miRNAs are shown in Figures S1 and S2. Four sites of *PABPN1* mRNA were chosen as targets for the hhRzs, namely, hhRz144, hhRz363, hhRz437, and hhRz867 were designed and tested in our recent publication.[31] In addition, six miRNAs were carefully designed using Invitrogen's RNAi designer.

We then inserted them in the GFP-miRNAi expression vector, suitable for transient and stable expression in cells. We employed the miRNA expression vector BLOCK-iT Pol II miR RNAi (Invitrogen, K4935-00) that allows the expression in mammalian cells of knockdown cassettes under the control of RNA polymerase II promoters. The use of a GFP-miRNA backbone vector (Figure S3) provides important advantages over shRNA vectors in minimizing the off-target possibility.[36] The DNA sequence of every plasmid containing hhRzs/miRNAs was confirmed using Sanger.

Developing the opt-PABPN1

We developed an opt-PABPN1 (GeneArt, Invitrogen) that is resistant to cleavage by hhRzs or miRNAs (Figure S8). The synthetic gene PAB_immune (Figure S9) (i.e., opt-PABPN1) was assembled from synthetic oligonucleotides and/or PCR products. The fragment was cloned into pMA-RQ (AmpR) using Sfil and Sfil-cloning sites. The plasmid DNA was purified from transformed bacteria, and the concentration was determined by UV spectroscopy. The final construct was verified by sequencing. Full sequence data and corresponding files were provided in CD-ROM from Invitrogen (Figures S8 and S9). PAB_immune was cut with EcoRI and BamHI from pMA-RQ plasmid and then ligated into GFP plasmid (opt-PABPN1-GFP) and Dsred plasmid (opt-PABPN1-Dsred).

PABPN1 Constructs

We used our previously constructed PABPN1 plasmids.[6,10]

Cell Culture and Transfection

24 h before transfection, transformed primary cell line (HEK293T) and HeLa cells were cultured in DMEM (Invitrogen) containing 10% fetal calf serum, while mouse myoblast cell line (C2C12) was cultured in DMEM containing 20% fetal calf serum. The stable C2C12 OPMD cell model was established in our recent publication.[9] Cells were grown in monolayer at 37°C in a cell culture incubator, with 5% CO_2 in 6-well plates and transfected at 70%–80% confluence. Transfection with 2 μg hhRz-containing plasmids and miRNA-containing plasmids was carried out using the Jet prime reagent (Polyplus-transfection, France), according to the manufacturer's protocol. For transfection experiments with individual hhRz or individual miRNA, control samples of nonsense hhRz or nonsense miRNA were used. For hhRz combination experiments, double the amount of control plasmid was used (i.e., 2× nonsense hhRz). Cells were routinely checked under fluorescent microscopy 24 h post-transfection for transfection efficiency. Stable clones of hhRzs and miRNAs were maintained in G418- (200 μg/mL) and blasticidin- (6 μg/mL) selective media, respectively. 1 week later, selected G418 and blasticidin cells were collected for RNA and protein extractions, in parallel, for further experiments.

Assessment of Cell Survival Using the Automated Live-Stage Microscope in a Stable C2C12 Muscle Cell Model for OPMD

We used the automated fluorescent microscope, as previously described,[9,10] and we calculated the percentage of cell survival in C2C12-17Ala myoblasts.[6,9]

Western Blotting

Total proteins were extracted in sodium dodecyl sulfate utilizing buffer (SUB) at different time points (containing 8M urea, 2% β-mercaptoethanol, and 0.5% SDS) and electrophoresed in 12% SDS-PAGE gels. Proteins were blotted on nitrocellulose membranes and probed with specific antibodies against PABPN1 (1:2,000) (Abcam, USA), Dsred (1:20) (Biovision, USA), and myosin (1:200) (DSHB, Iowa City, IA, USA). Parallel samples were probed using monoclonal actin antibody (Chemicon International, USA) to confirm the equal loading of lysates between lanes. After incubation with specific secondary horseradish peroxidase (HRP)-conjugated antibodies, the membranes were revealed using the western blot chemiluminescence reagent plus kit (NEN Life Sciences Products, Boston, MA, USA).

qPCR

Total RNA (200 ng) was extracted from transfected cells by Trizol (Ambion), according to the manufacturer's instructions. cDNA was synthesized using the SuperScript Vilo (Thermo Fisher Scientific) and mixed with the PABPN1 probe (Applied Biosystems), following the manufacturer's instructions. RNA polymerase II was used as an internal control. All qPCR experiments were conducted at 50°C for 2 min, 95°C for 10 min, and then 40 cycles of 95°C for 15 s and 60°C for 1 min. The specificity of the reaction was verified by melt curve analysis. The reaction was performed in triplicate. The threshold crossing value was noted for each transcript and normalized to the internal control. The relative quantitation of each mRNA was performed using the comparative Ct method. Experiments were performed using QuantStudio Real-time PCR system (Applied Biosystems), and data processing was performed using QuantStudio Real-time PCR software (Applied Biosystems), using a probe and a set of primers specific for opt-PABPN1 as well as a different probe and a set of primers specific for wild-type PABPN1.

The sequence of opt-PABPN1's probe was 5′-TCCAGGCGGAGC TGGCGATTAT-3′, while the sequence of wild-type PABPN1's probe was 5′-TCGAGGGTGACCCGGGGGA-3′ (TaqMan Gene Expression Assays PABPN1, Applied Biosystems). To confirm the qPCR results, we also used the following primers to amplify opt-PABPN1:

Forward 1 5′-AGAAAGCGTGCGGACCAG-3′

Reverse 1 5′-GAGCCACAAGCTGGTACA-3′

Also, the following primers were used to amplify wild-type PABPN1:

Forward 2 5′-ATGGTGCAACAGCAGAAGAG-3′

Reverse 2 5′-CAGCTCCCGCTCTCGATTCT-3′

ELISA

Transfected cells were collected to determine the concentration of PABPN1. An ELISA kit (Promega) was used for quantitative measurement, following the manufacturer's recommendations. All samples were assayed in duplicate on each plate. The optical density of each well was measured using Spectramax plate reader (Bio-Rad).

hhRz Design for *C. elegans*, Worm Strains and Maintenance, Western Blot Analysis, Zeiss Microscopy, and Motility Measurements

Standard methods for culturing and handling the worms were used.[47] Worms were cultured on standard nematode growth media (NGM) streaked with the OP-50 *Escherichia coli* strain at 20°C if not specified otherwise. Transgenic *C. elegans* expressing human PABPN1 with 0 and 13 alanines[8] were used. All constructs were sequenced to confirm their integrity.

Three lines derived from hhRz144, hhRz363, and hhRz437 *C. elegans* plasmids were generated by Knudra Transgenics (Murray, UT, USA). First, we constructed each of the three hhRzs in an appropriate *C. elegans* plasmid. We then sent the constructs to Knudra Transgenics (Murray, UT, USA) where MosSCI transgenics were done by transgenic capture. Transgene injection was done by inserting DNA mixes into the gonad of the model organism, and transgenics selection was done by screening strains by PCR for single-copy insertion at the mos1 locus. Genotypes of animals expressing PABPN1 and hhRzs were verified using the *PABPN1* primers and hhRz primers, respectively. To test for PABPN1 expression levels, proteins from fourth larval stage (L4) larvae were extracted as described.[48]

For visualizing the green fluorescent signal in worms, the worms were immobilized in M9 worm buffer with 5 mM levamisole and mounted on slides with 2% agarose pads. GFP was visualized using the Zen Pro 2012.SD/total internal reflection fluorescence (TIRF) Zeiss AxioObserver (Acquisition Fluorescence, TIRF, charge-coupled device [CCD] AxioCam MRm camera) was used (1,388 × 1,040 pixels) and the light source was an Xcite 120Q lamp with appropriate filter cubes to detect GFP. All images were acquired with the Zen Blue software. Stitching and/or maximum-intensity projections were done for all tile and/or z stack images).

For motility of the nematode, a synchronized worm population was obtained using hypochlorite extraction. Worms were grown on solid media up to day 1 of adulthood. At day 1, 30 worms/well were placed in S basal with OP-50 *Escherichia coli* (optical density 0.5) in a flat-bottom 96-well plate; at least 3 wells were done per condition. PABPN1-13Ala worms crossed with hhRz144, hhRz363, or hhRz437 as well as the controls (non-crossed PABPN1-13Ala animals and PABPN1-0Ala) were let to rest in the dark for 1 h before recording their motility. We then used the 96-well-based infrared locomotor tracking system known as the Microtracker (Phylumtech, Santa Fe, Argentina) method to detect the motion of the worms on a continuous basis. The system detects animal movement through infrared microbeam light scattering. Briefly, each microtiter well is crossed by at least one infrared microbeam, scanned more than 10 times/s. The detected signal is then digitally processed to register the amount of animal movement in a fixed period of time. For any plate, the system allowed us to set groups of replicate wells; in this way, the software informs the activity of each well and the average activity of the group. At the end of each run, the system generated reports with the activity over time of each replicate group, well, and channel. The detected signal is then digitally processed to register the amount of animal movement in a fixed period of time.

Statistical Analysis

All values represent the mean of at least three independent experiments (mean ± SE). Statistical differences between hhRz/miRNA treatment and control groups were evaluated by the Student's t test (for comparisons of two groups) and the ANOVA (for multiple group comparisons). In every analysis, values of $^{*}p < 0.05$ compared with any other groups were designated as statistically significant.

SUPPLEMENTAL INFORMATION

Supplemental Information includes eighteen figures and three tables and can be found with this article online at https://doi.org/10.1016/j.omtn.2019.02.003.

AUTHOR CONTRIBUTIONS

A.A.-B. performed the majority of the experiments, analyzed the data, and wrote the manuscript. N.K. conceived the study; designed and constructed the hhRzs, miRNAs, and the opt-PABPN1; and revised the manuscript. J.P. helped in hhRz design and revised the manuscript. A.G. carried out the worm genotypes and matings. M.S. helped in hhRz construction. C.M. helped in *C. elegans* microscopy images and Microtracker experiments. M.D. helped in western blot. C.N. provided the *C. elegans* strains of OPMD. P.A.D. revised the first and final drafts of the manuscript. A.P. provided the Microtracker and Zeiss used for the *C. elegans* experiments and revised the manuscript. L.V. designed hhRz worms and helped in miRNA and opt-PABPN1 design. G.A.R. supervised the study and revised the manuscript.

CONFLICTS OF INTEREST

The authors declare no conflicts of interest.

ACKNOWLEDGMENTS

We thank Dr. Helene Catoire and Dr. Martine Therrien for their technical support on *C. elegans*. This work was supported by the Canadian Institutes of Health Research (CIHR) operating grant: Characterization of PABPN1 for the development of an OPMD treatment (JNM-85075), Muscular Dystrophy Canada, the Muscular Dystrophy Association, (MDA) United States, and the Federation Foundation of Greater Philadelphia.

REFERENCES

1. Dion, P., Shanmugam, V., Gaspar, C., Messaed, C., Meijer, I., Toulouse, A., Laganiere, J., Roussel, J., Rochefort, D., Laganiere, S., et al. (2005). Transgenic expression of an expanded (GCG)13 repeat PABPN1 leads to weakness and coordination defects in mice. Neurobiol. Dis. *18*, 528–536.
2. Shanmugam, V., Dion, P., Rochefort, D., Laganière, J., Brais, B., and Rouleau, G.A. (2000). PABP2 polyalanine tract expansion causes intranuclear inclusions in oculopharyngeal muscular dystrophy. Ann. Neurol. *48*, 798–802.
3. Tomé, F.M., and Fardeau, M. (1980). Nuclear inclusions in oculopharyngeal dystrophy. Acta Neuropathol. *49*, 85–87.
4. Brais, B., Bouchard, J.P., Xie, Y.G., Rochefort, D.L., Chrétien, N., Tomé, F.M., Lafrenière, R.G., Rommens, J.M., Uyama, E., Nohira, O., et al. (1998). Short GCG expansions in the PABP2 gene cause oculopharyngeal muscular dystrophy. Nat. Genet. *18*, 164–167.
5. Brais, B., Xie, Y.G., Sanson, M., Morgan, K., Weissenbach, J., Korczyn, A.D., Blumen, S.C., Fardeau, M., Tomé, F.M., Bouchard, J.P., et al. (1995). The oculopharyngeal muscular dystrophy locus maps to the region of the cardiac alpha and beta myosin heavy chain genes on chromosome 14q11.2-q13. Hum. Mol. Genet. *4*, 429–434.
6. Abu-Baker, A., Kharma, N., Neri, C., Rasheed, S., Dion, P.A., Varin, L., and Rouleau, G.A. (2016). Current targeted therapeutic strategies for oculopharyngeal muscular dystrophy: from pharmacological to RNA replacement and gene editing therapies. Int. J. Clin. Neurosci. Ment. Health *3* (*Suppl 1*), S06.
7. Abu-Baker, A., Messaed, C., Laganiere, J., Gaspar, C., Brais, B., and Rouleau, G.A. (2003). Involvement of the ubiquitin-proteasome pathway and molecular chaperones in oculopharyngeal muscular dystrophy. Hum. Mol. Genet. *12*, 2609–2623.
8. Catoire, H., Pasco, M.Y., Abu-Baker, A., Holbert, S., Tourette, C., Brais, B., Rouleau, G.A., Parker, J.A., and Néri, C. (2008). Sirtuin inhibition protects from the polyalanine muscular dystrophy protein PABPN1. Hum. Mol. Genet. *17*, 2108–2117.
9. Abu-Baker, A., Parker, A., Ramalingam, S., Laganiere, J., Brais, B., Neri, C., Dion, P., and Rouleau, G. (2018). Valproic acid is protective in cellular and worm models of oculopharyngeal muscular dystrophy. Neurology *91*, e551–e561.
10. Abu-Baker, A., Laganiere, J., Gaudet, R., Rochefort, D., Brais, B., Neri, C., Dion, P.A., and Rouleau, G.A. (2013). Lithium chloride attenuates cell death in oculopharyngeal muscular dystrophy by perturbing Wnt/β-catenin pathway. Cell Death Dis. *4*, e821.
11. Fan, X., Dion, P., Laganiere, J., Brais, B., and Rouleau, G.A. (2001). Oligomerization of polyalanine expanded PABPN1 facilitates nuclear protein aggregation that is associated with cell death. Hum. Mol. Genet. *10*, 2341–2351.
12. Abu-Baker, A., Laganiere, S., Fan, X., Laganiere, J., Brais, B., and Rouleau, G.A. (2005). Cytoplasmic targeting of mutant poly(A)-binding protein nuclear 1 suppresses protein aggregation and toxicity in oculopharyngeal muscular dystrophy. Traffic *6*, 766–779.
13. Wang, Q., Mosser, D.D., and Bag, J. (2005). Induction of HSP70 expression and recruitment of HSC70 and HSP70 in the nucleus reduce aggregation of a polyalanine expansion mutant of PABPN1 in HeLa cells. Hum. Mol. Genet. *14*, 3673–3684.
14. Chartier, A., Raz, V., Sterrenburg, E., Verrips, C.T., van der Maarel, S.M., and Simonelig, M. (2009). Prevention of oculopharyngeal muscular dystrophy by muscular expression of Llama single-chain intrabodies in vivo. Hum. Mol. Genet. *18*, 1849–1859.
15. Verheesen, P., de Kluijver, A., van Koningsbruggen, S., de Brij, M., de Haard, H.J., van Ommen, G.J., van der Maarel, S.M., and Verrips, C.T. (2006). Prevention of oculopharyngeal muscular dystrophy-associated aggregation of nuclear polyA-binding protein with a single-domain intracellular antibody. Hum. Mol. Genet. *15*, 105–111.
16. Davies, J.E., Rose, C., Sarkar, S., and Rubinsztein, D.C. (2010). Cystamine suppresses polyalanine toxicity in a mouse model of oculopharyngeal muscular dystrophy. Sci. Transl. Med. *2*, 34ra40.
17. Davies, J.E., Sarkar, S., and Rubinsztein, D.C. (2006). Trehalose reduces aggregate formation and delays pathology in a transgenic mouse model of oculopharyngeal muscular dystrophy. Hum. Mol. Genet. *15*, 23–31.
18. Davies, J.E., Wang, L., Garcia-Oroz, L., Cook, L.J., Vacher, C., O'Donovan, D.G., and Rubinsztein, D.C. (2005). Doxycycline attenuates and delays toxicity of the oculopharyngeal muscular dystrophy mutation in transgenic mice. Nat. Med. *11*, 672–677.
19. Périé, S., Trollet, C., Mouly, V., Vanneaux, V., Mamchaoui, K., Bouazza, B., Marolleau, J.P., Laforêt, P., Chapon, F., Eymard, B., et al. (2014). Autologous myoblast transplantation for oculopharyngeal muscular dystrophy: a phase I/IIa clinical study. Mol. Ther. *22*, 219–225.
20. Malerba, A., Klein, P., Bachtarzi, H., Jarmin, S.A., Cordova, G., Ferry, A., Strings, V., Espinoza, M.P., Mamchaoui, K., Blumen, S.C., et al. (2017). PABPN1 gene therapy for oculopharyngeal muscular dystrophy. Nat. Commun. *8*, 14848.
21. Bao, Y.P., Cook, L.J., O'Donovan, D., Uyama, E., and Rubinsztein, D.C. (2002). Mammalian, yeast, bacterial, and chemical chaperones reduce aggregate formation and death in a cell model of oculopharyngeal muscular dystrophy. J. Biol. Chem. *277*, 12263–12269.
22. Barbezier, N., Chartier, A., Bidet, Y., Buttstedt, A., Voisset, C., Galons, H., Blondel, M., Schwarz, E., and Simonelig, M. (2011). Antiprion drugs 6-aminophenanthridine and guanabenz reduce PABPN1 toxicity and aggregation in oculopharyngeal muscular dystrophy. EMBO Mol. Med. *3*, 35–49.
23. Argov, Z., Gliko-Kabir, I., Brais, B., Caraco, Y., and Megiddo, D. (2016). Intravenous Trehalose Improves Dysphagia and Muscle Function in Oculopharyngeal Muscular Dystrophy (OPMD): Preliminary Results of 24 Weeks Open Label Phase 2 Trial (S28.004). Neurology *86* (16 Suppl), S28.004.
24. Zhang, Y.C., Taylor, M.M., Samson, W.K., and Phillips, M.I. (2005). Antisense inhibition: oligonucleotides, ribozymes, and siRNAs. Methods Mol. Med. *106*, 11–34.
25. Citti, L., and Rainaldi, G. (2005). Synthetic hammerhead ribozymes as therapeutic tools to control disease genes. Curr. Gene Ther. *5*, 11–24.
26. Ren, A., Micura, R., and Patel, D.J. (2017). Structure-based mechanistic insights into catalysis by small self-cleaving ribozymes. Curr. Opin. Chem. Biol. *41*, 71–83.
27. Macfarlane, L.A., and Murphy, P.R. (2010). MicroRNA: Biogenesis, Function and Role in Cancer. Curr. Genomics *11*, 537–561.
28. Montano, M. (2011). MicroRNAs: miRRORS of health and disease. Transl. Res. *157*, 157–162.
29. Bartel, D.P. (2004). MicroRNAs: genomics, biogenesis, mechanism, and function. Cell *116*, 281–297.
30. Jonas, S., and Izaurralde, E. (2015). Towards a molecular understanding of microRNA-mediated gene silencing. Nat. Rev. Genet. *16*, 421–433.
31. Kharma, N., Varin, L., Abu-Baker, A., Ouellet, J., Najeh, S., Ehdaeivand, M.R., Belmonte, G., Ambri, A., Rouleau, G., and Perreault, J. (2016). Automated design of hammerhead ribozymes and validation by targeting the PABPN1 gene transcript. Nucleic Acids Res. *44*, e39.
32. Blumen, S.C., Korczyn, A.D., Lavoie, H., Medynski, S., Chapman, J., Asherov, A., Nisipeanu, P., Inzelberg, R., Carasso, R.L., Bouchard, J.P., et al. (2000). Oculopharyngeal MD among Bukhara Jews is due to a founder (GCG)9 mutation in the PABP2 gene. Neurology *55*, 1267–1270.
33. Rodríguez, M., Camejo, C., Bertoni, B., Braida, C., Rodríguez, M.M., Brais, B., Medici, M., and Roche, L. (2005). (GCG)11 founder mutation in the PABPN1 gene of OPMD Uruguayan families. Neuromuscul. Disord. *15*, 185–190.
34. Rivera, D., Mejia-Lopez, H., Pompa-Mera, E.N., Villanueva-Mendoza, C., Nava-Castañeda, A., Garnica-Hayashi, L., Cuevas-Covarrubias, S., and Zenteno, J.C. (2008). Two different PABPN1 expanded alleles in a Mexican population with oculopharyngeal muscular dystrophy arising from independent founder effects. Br. J. Ophthalmol. *92*, 998–1002.

35. Marusin, A.V., Kurtanov, KhA., Maksimova, N.R., Svarovskaya, M.G., and Stepanov, V.A. (2016). [Haplotype Analysis of Oculopharyngeal Muscular Dystrophy (OPMD) Locus in Yakutia]. Genetika *52*, 376–384.

36. Boudreau, R.L., Martins, I., and Davidson, B.L. (2009). Artificial microRNAs as siRNA shuttles: improved safety as compared to shRNAs in vitro and in vivo. Mol. Ther. *17*, 169–175.

37. Davies, J.E., Sarkar, S., and Rubinsztein, D.C. (2008). Wild-type PABPN1 is anti-apoptotic and reduces toxicity of the oculopharyngeal muscular dystrophy mutation. Hum. Mol. Genet. *17*, 1097–1108.

38. Wahle, E., Lustig, A., Jenö, P., and Maurer, P. (1993). Mammalian poly(A)-binding protein II. Physical properties and binding to polynucleotides. J. Biol. Chem. *268*, 2937–2945.

39. Messaed, C., Dion, P.A., Abu-Baker, A., Rochefort, D., Laganiere, J., Brais, B., and Rouleau, G.A. (2007). Soluble expanded PABPN1 promotes cell death in oculopharyngeal muscular dystrophy. Neurobiol. Dis. *26*, 546–557.

40. Krause, S., Fakan, S., Weis, K., and Wahle, E. (1994). Immunodetection of poly(A) binding protein II in the cell nucleus. Exp. Cell Res. *214*, 75–82.

41. Kole, R., Krainer, A.R., and Altman, S. (2012). RNA therapeutics: beyond RNA interference and antisense oligonucleotides. Nat. Rev. Drug Discov. *11*, 125–140.

42. Li, C., Xiao, P., Gray, S.J., Weinberg, M.S., and Samulski, R.J. (2011). Combination therapy utilizing shRNA knockdown and an optimized resistant transgene for rescue of diseases caused by misfolded proteins. Proc. Natl. Acad. Sci. USA *108*, 14258–14263.

43. Phylactou, L.A., Kilpatrick, M.W., and Wood, M.J. (1998). Ribozymes as therapeutic tools for genetic disease. Hum. Mol. Genet. *7*, 1649–1653.

44. Jazurek, M., Ciesiolka, A., Starega-Roslan, J., Bilinska, K., and Krzyzosiak, W.J. (2016). Identifying proteins that bind to specific RNAs - focus on simple repeat expansion diseases. Nucleic Acids Res. *44*, 9050–9070.

45. Jaworska, E., Kozlowska, E., Switonski, P.M., and Krzyzosiak, W.J. (2016). Modeling simple repeat expansion diseases with iPSC technology. Cell. Mol. Life Sci. *73*, 4085–4100.

46. Costa, Mdo.C., Luna-Cancalon, K., Fischer, S., Ashraf, N.S., Ouyang, M., Dharia, R.M., Martin-Fishman, L., Yang, Y., Shakkottai, V.G., Davidson, B.L., et al. (2013). Toward RNAi therapy for the polyglutamine disease Machado-Joseph disease. Mol. Ther. *21*, 1898–1908.

47. Stiernagle, T. (2006). Maintenance of C. elegans. WormBook *2006*, 1–11.

48. Berdichevsky, A., Viswanathan, M., Horvitz, H.R., and Guarente, L. (2006). C. elegans SIR-2.1 interacts with 14-3-3 proteins to activate DAF-16 and extend life span. Cell *125*, 1165–1177.